IEEE Access
Multidisciplinary | Rapid Review | Open Access Journal

Date of publication xxxx 00, 0000, date of current version xxxx 00, 0000.

Digital Object Identifier 10.1109/ACCESS.2017.Doi Number

Metrological performance of hybrid measurement technique applied for the Lamb waves phase velocity dispersion evaluation

L. Draudviliene[1], A. Meskuotiene[2], O. Tumsys[1], L. Mazeika[1], V. Samaitis[1]

[1]Kaunas University of Technology, Ultrasound Institute,Kaunas, Lithuania
[2]Kaunas University of Technology, Metrology Institute, Kaunas, Lithuania

Corresponding author: First Author (e-mail: lina.draudviliene@ ktu.lt).

ABSTRACT The work presents the metrological evaluation of the modify hybrid spectrum decomposition and zero-crossing technique. The presented technique enables to reconstruct the phase velocity dispersion curve part of Lamb wave modes using only two signals. This is set to consequently simplify the of complex guided wave signals analysis. Experimentally measured asymmetric A_0 mode Lamb wave signals propagating in 4 mm thickness non-homogeneous Glass Fibre Reinforced Plastic (GFRP) plate are used for assessment of the proposed technique. The phase velocity dispersion curve (DC) segments are obtained using three different filter bandwidths as reference using the DC obtained by the semi-analytical finite element method SAFE. The proposed technique quantitative and qualitative characteristics are presented. Using this technique and employing various band-pass filters it is shown that the DC segments are reconstructed in approximately 50% - 88% bandwidth of the incident signal frequency spectrum. The average of the calculated expanded uncertainties for all filter bandwidths is equal to approximately 2%. The narrower filter bandwidth has produced smaller systematic errors equal to 1.8%, yielding to wider reconstructed dispersion curve segments.

INDEX TERMS composite plate, dispersion curves, Lamb waves, phase velocity, reliability, uncertainty quantification

I. INTRODUCTION

In recent years, the ultrasonic guided waves (UGW) are used in many industrial fields and applications due to possibility to detect defects and delaminations and to evaluate their parameters in large structures. By analyzing the amplitude or variation of propagation velocity of these waves, the non-homogeneities which may be available on objects with various geometries and properties can be detected [1]-[9]. Therefore, guided wave inspection is a convenient tool for the evaluation of the non-homogeneities in composite materials owing to sensitivity of propagation velocity to the material surface and internal defects and capability to propagate long distances with reasonable attenuation [10]-[15]. However, guided waves possess a dispersion phenomenon, a multi – mode character and conversion to other modes on the boundaries of non-uniformities [14], [16]-[20]. The dispersion phenomenon leads to presence of two types of interrelated velocities - phase and group, both frequencies dependent and characterized by dispersion curves [21]-[22]. As the different frequency components propagate with different velocities after some distance they are concentrated in different UGW signal parts in the time domain [23]. This leads to the change of the waveform, elongation in time and reduction of the amplitude [1], [24]-[25].

The incidence of many modes at the same frequency band with similar signal amplitudes [26] complicates the identification of the particular signal under interest. The multi-modal behavior of guided waves exists in any case even in the case of single mode excitation techniques, as any imperfection in the structure may cause at least one conversion of guided wave modes. Such complex features of the guided waves generate hurdles to identify the required signal and to determine accurately the amplitudes of the signal and/or propagation velocities [27]. Therefore, in order to use effectively the UGW in non-destructive applications, it is necessary to reconstruct the dispersion curves of group and/or phase velocities by extracting the time and frequency

information from these complicated signals. The reconstructed dispersion curves allow identifying different modes in complex trails of the signal. Identification of different modes offers the possibility to determine more accurately the defect location and size and/or estimation of the material properties [11]. To resolve these tasks, the hybrid spectrum decomposition and zero-crossing technique for the evaluation of phase velocity dispersion relations of the Lamb wave's fundamental modes presented in previous work was proposed [28]. This technique has been verified in two different conditions:

a) On a homogenous medium using simulated and experimental signals of aluminum plate.

b) On a non – homogeneous medium using signals obtained by 3D finite element model of Carbon Fiber Reinforced Plastic (CFRP) plate.

In both cases, the obtained results have indeed verified suitability the proposed hybrid measurement technique to evaluate the Lamb waves phase velocity dispersion properties and to reconstruct the segment of dispersion curve. However, any measurement would be incomplete without an associated uncertainty to go along with. It is an important aspect of measurements that would affect costs, quality, and risks of the taken decisions. Therefore, to apply this presented hybrid technique in future investigations its reliability is needed to be evaluated. It has been reported in a previous study [28] that all stages of this method influence the measurement uncertainties. To evaluate a set of factors affecting the quality of experimental results the systematic and random errors are analyzed. These errors are quantified using conventional analytic methods and Monte Carlo simulation. The obtained experimental errors are combined with other unobserved sources of uncertainties, known using some other means. The estimation process of the measurement uncertainty includes the grouping sources covered by existing data, quantifying of the grouped and remaining components, converting these components to standard deviations.

This work aim is to evaluate the accuracy of the proposed hybrid spectrum decomposition and zero-crossing technique in Lamb wave's applications. To achieve this goal, the quantitative and qualitative characteristics of the method have been assessed based on the calculation of the systematic and random errors, the expanded uncertainty and the determination of the main uncertainty components influenced by the measurement result.

The investigation consists then in two main stages: the experimental investigation and the hybrid technique reliability evaluation. At first, the measurement object, the experimental set-up and the hybrid technique are described. Then the phase velocity dispersion curve segments of A_0 mode are obtained using hybrid technique and SAFE method as reference. Secondly, the evaluation uncertainties of the proposed hybrid technique are analyzed and assessed.

II. EXPERIMENTAL INVESTIGATION

A. MEASUREMENT OBJECT

The composite GFRP plate is selected as an object of investigation. Such composites are widely used in many industrial applications, such as the manufacturing of the bodies of buses, ships, and wind power wings etc. [29]-[31].The selected GFRP laminate consists of six layers with ply orientations of -45^0 and $+45^0$ degrees yielding to overall plate thickness of d=4 mm (Fig. 1).

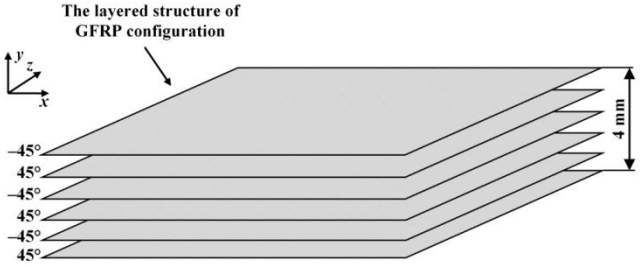

FIGURE 1. The configuration of the GFRP plate is used in the investigation.

The semi-analytical finite element (SAFE) method [10], [32] has been used for the theoretical dispersion curves calculation. The elastic properties [33] of the investigated object are presented in Table 1, where the axis x, y, z are marked accordingly as 2, 3, 1. In this case, a generalized stiffness matrix was used to describe a GFRP laminate [34]. Hence, the stiffness matrix was obtained by summing the contribution of each ply in terms of their respective thicknesses. The obtained Lamb waves fundamental A_0 and S_0 modes phase velocity dispersion curves with SAFE method are presented in Fig. 2.

TABLE 1. The elastic coefficients of the glass fiber reinforced plastic (GFRP) plate.

Material	E_1, GPa	E_2, GPa	ν_{12}	ν_{23}	G_{12}, GPa	ρ, kg/m^3
GFRP	27.1	12.1	0.18	0.2	4.1	1960

This article has been accepted for publication in a future issue of this journal, but has not been fully edited. Content may change prior to final publication. Citation information: DOI 10.1109/ACCESS.2020.2974586, IEEE Access

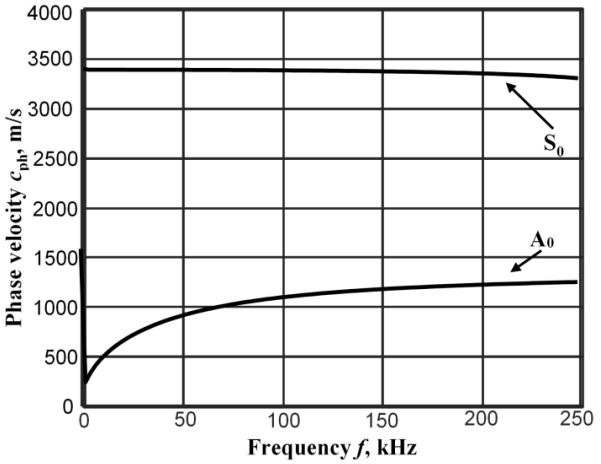

FIGURE 2. The Lamb waves A_0 and S_0 modes phase velocity dispersion curves obtained with SAFE method.

As it can be seen in Fig. 2, the asymmetric A_0 mode possesses a big dispersion nature especially in lower frequency bandwidth, while the symmetric S_0 mode is almost non-dispersive in frequency ranges under analysis.

There are mainly two parameters – the velocity and the amplitude of the signal used in the non-destructive evaluations and/or in monitoring applications. According to the UGW phase velocity, frequency and peak amplitude variations, the location and the size of the defect such as delamination can be detected [11]. Therefore, it is necessary to reconstruct dispersion curves from the signals acquired on the object under investigation.

B. EXPERIMENTAL SET-UP

To investigate the feasibility of proposed dispersion curve reconstruction technique, experiments have been carried out on GFRP sample, possessing the geometry and sensor allocation, as shown in Fig. 3. Throughout the experiments, the custom-made thickness mode actuator was mounted on top of the sample. To get the reliable acoustic contact between the sensor and the specimen, a glass textolite protector with a contact area of 3 mm^2 and a thin layer of glycerol was used. An actuator was driven with a 3 cycle, 200 V square pulses with a central frequency of 130 kHz, to generate multiple modes in wide frequency bandwidth. To collect the experimental data, the same type of transducer was attached perpendicularly to the surface of the sample and scanned along the straight wave path of guided waves. The receiver was moved away from the transmitter up to 600 mm with a step increment 0.5 mm. The initial spacing between the actuator and sensor was equal to 100 mm. The waveforms were recorded using a 50 MHz sampling frequency. The response signals at each position were measured 8 times and averaged to ensure better signal to noise ratio. In this way, the B-scan dataset of out-of-plane component was collected at the centerline of the sample. The experimental set-up is graphically pointed up at Fig. 3; the B-scan image of the Lamb waves A_0 mode signals is presented in Fig. 4.

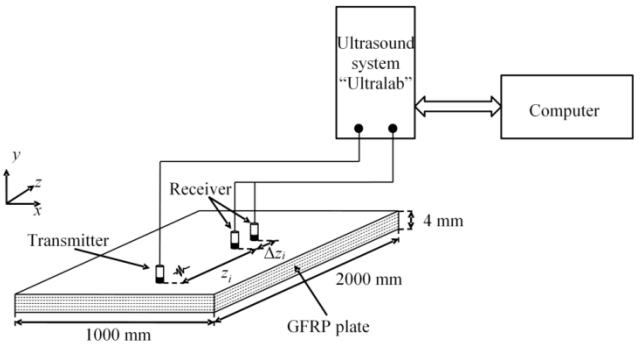

FIGURE 3. The experimental set-up for phase velocity measurement of the Lamb waves A_0 and S_0 modes propagating in 4 mm thickness multilayer GFRP sample.

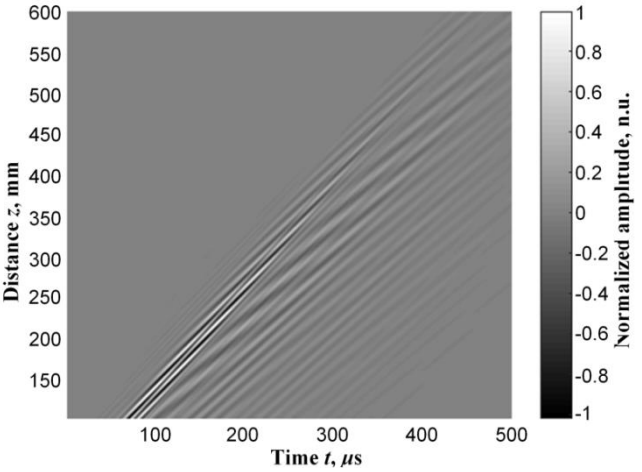

FIGURE 4. The B–scan image of the Lamb wave signals measured on the 4 mm thickness GFRP plate.

The B-scan data was required just to have general view of propagating waves. The proposed hybrid technique uses only a pair of the B-scan signals. The use of these two signals measured at different positions essentially simplifies the approach and makes it suitable for structural health monitoring applications. So, from now on only one pair of the signals recorded at the receiver position 150 mm and 155 mm will be used. For the processing of the selected signals, the technique is used. A brief description of this technique is presented in the next section.

C. BRIEF DESCRIPTION OF THE HYBRID TECHNIQUE

The proposed hybrid technique combines two approaches: the zero-crossing method and the spectrum decomposition method (Fig. 5). At first, these methods were used separately to evaluate the Lamb waves phase velocity (zero-crossing method) [35] and group velocity (spectrum decomposition method) [36] dispersion characteristics and to reconstruct the dispersion curve segments. The uncertainty quantification for both techniques has been completed accordingly to previous works [37], [38]. The investigations have confirmed that both

This article has been accepted for publication in a future issue of this journal, but has not been fully edited. Content may change prior to final publication. Citation information: DOI 10.1109/ACCESS.2020.2974586, IEEE Access

methods are suitable for the Lamb wave applications. As regards the hybrid technique basics, mathematical description and suitability for the Lamb wave's dispersion evaluation are also available in earlier work [28]. The block diagram of the proposed hybrid method for the estimation of the phase velocity of the guided waves exploiting the signals measured at two different spatial positions is presented in Fig. 5 and briefly described below.

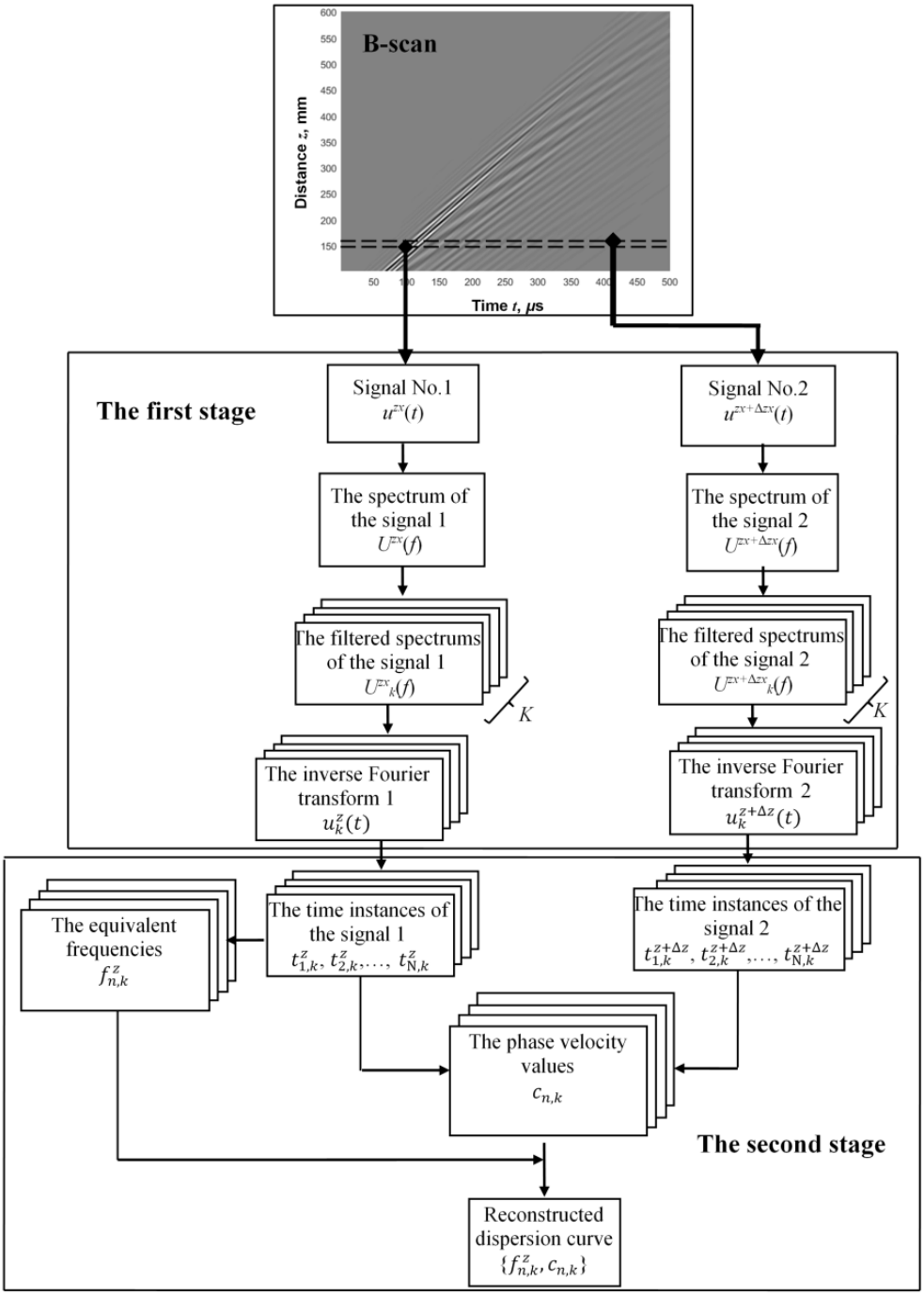

FIGURE 5. The block diagram based on the spectrum decomposition and zero-crossing approaches for the Lamb waves phase velocity reconstruction using signals measured at two different spatial positions.

This article has been accepted for publication in a future issue of this journal, but has not been fully edited. Content may change prior to final publication. Citation information: DOI 10.1109/ACCESS.2020.2974586, IEEE Access

According to the presented block diagram (Fig. 5), in the first stage the spectrum decomposition approach is used [28]:

- Two signals at two different spatial positions $u^z(t)$, $u^{z+\Delta z}(t)$ are recorded, where Δz is the distance between two signals;
- The frequency spectra of these two signals are calculated using the Fourier transform $U^z(f)$, $U^{z+\Delta z}(f)$;
- The frequency spectra of these two signals are filtered using K bandpass Gaussian filters:

$$B_k(f) = e^{4\ln(0.5)\left(\frac{f-f_L-(k-1)df}{\Delta B}\right)^2}, \quad (1)$$

where k=1,2,...K, is the number of the bandpass filter, K is the total number of filters:

$$K \geq \frac{f_H - f_L}{\Delta B} + 1, \quad (2)$$

f_L and f_H are the frequency ranges in which the central frequencies of the filters are varied with step df, ΔB is the filter bandwidth at -6 dB level;

- The step in a frequency domain between central frequencies of such signals is calculated according to the expression presented by Ping He [39]:

$$df = \frac{f_H - f_L}{K-1}; \quad (3)$$

- The filtered signals are reconstructed back to the time domain using the inverse Fourier transform.

In the second stage, for each pair of the filtered signals the zero-crossing approach is used [19]:

- According to the chosen threshold level U_{th} the multiple zero-crossing time instances at which the signals crosses the zero amplitude line are estimated in the each of the filtered signal $t^z_{1,k}, t^z_{2,k}, \dots, t^z_{N,k}$ and $t^{z+\Delta z}_{1,k}, t^{z+\Delta z}_{2,k}, \dots, t^{z+\Delta z}_{N,k}$,where N is the total number of measured zero-crossing instances in the signal;
- The phase velocity is estimated using time difference between corresponding zero-crossing instances in the signals measured at two different spatial position signals [37]:

$$c_{n,k} = \frac{\Delta z}{t^{z+\Delta z}_{n,k} - t^z_{n,k}}; \quad (4)$$

- The equivalent frequencies $f^x_{n,k}$ of the filtered first signals $u^x_k(t)$ are calculated by:

$$f^z_{n,k} = \frac{1}{2\cdot\left(t^z_{n+1,k} - t^z_{n,k}\right)}; \quad (5)$$

- The segment of the phase velocity dispersion curves $\{f^z_{n,k}, c_{n,k}\}$ is determined by creating sets of pairs of estimated equivalent frequencies $f^z_{n,k}$ and phase velocities $c_{n,k}$.

Using such algorithm, the processing of the selected two signals is then performed and the obtain results are presented in the next section.

D. EVALUATION OF THE PHASE VELOCITY DISPERSION

To obtain the Lamb wave phase velocity dispersion curves the proposed hybrid technique is applied. For this technique some significant parameters are needed to be determined [22] and they are resulted from the signal frequency spectrum. The signal at distance 150 mm and its frequency spectrum are presented in Fig. 6(a) and Fig. 6(b).

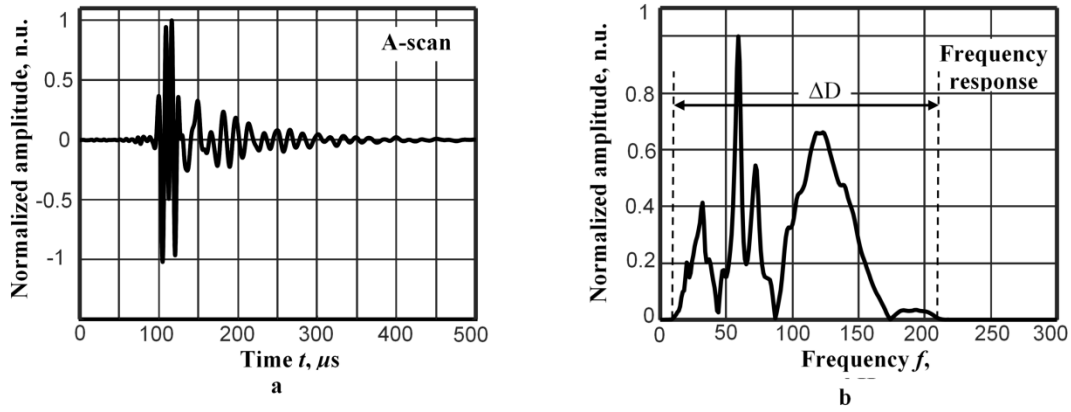

FIGURE 6. **TheLamb wave A_0 mode waveform of the signal at 150 mm distance (a) and the frequency response of this signal (b)**

According to the A_0 mode signal frequency spectrum (Fig. 6(b)) the bandwidth at -40 dB level is in the range of 10-210 kHz. Therefore, the frequency range for the filtering is chosen according to these parameters, which means that the reconstructed phase velocity dispersion curve should cover this frequency range. In order, to assess this statement the proposed method was investigated using three different band-pass filters applied for spectrum decomposition. The bandwidth of band-pass filters was set to ΔB_1=25 kHz, ΔB_2=50 kHz and ΔB_3=75 kHz. Such bandwidths were selected taking into the account the frequency bandwidth of the analyzed signal, which is ΔD=200 kHz at -40dB. The number of filters K for spectrum decomposition is calculated according to the Eq.(2) taking into account the selected filter bandwidth ΔB. In the case of 25 kHz, 50 kHz and 75 kHz filter bandwidth ΔB the corresponding number of filters was K=10, K=5 and K=4. The measurement results using different filters bandwidth and different sets of the filters are compared with

This article has been accepted for publication in a future issue of this journal, but has not been fully edited. Content may change prior to final publication. Citation information: DOI 10.1109/ACCESS.2020.2974586, IEEE Access

the dispersion curve obtained by SAFE method (Fig. 7). The main parameters of the reconstructed A_0 mode phase velocity dispersion curves are presented in the Table 2.

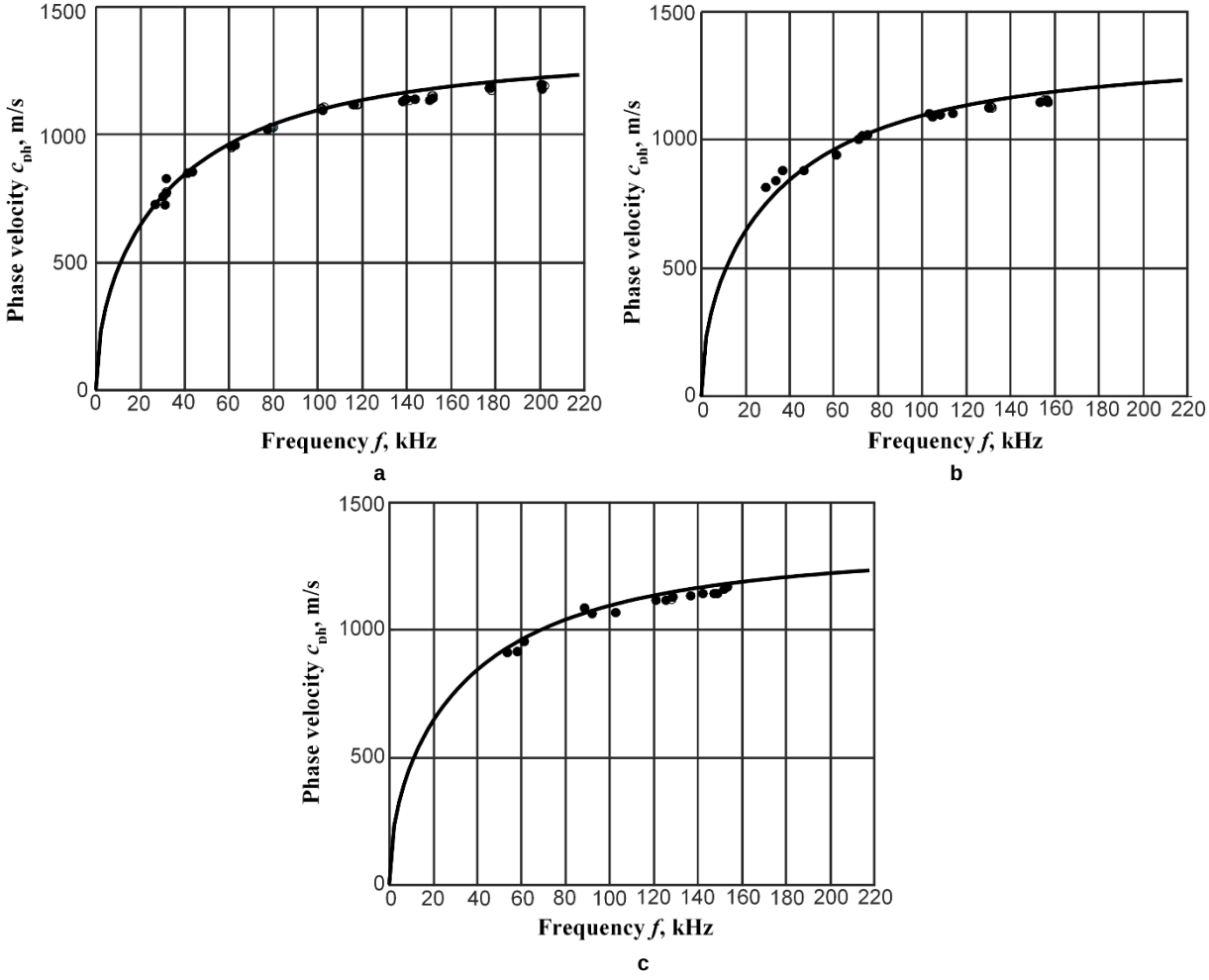

FIGURE 7. **Reconstructed phase velocities dispersion curves of the Lamb wave A_0 mode: theoretical dispersion curve (*solid line*) calculated using SAFE method, measured values (*dots*): a – obtained with hybrid algorithm using 10 bandpass Gaussian filters (the bandwidth of the each filter ΔB=25 kHz); b – obtained with proposed algorithm using 5 filters (ΔB=50 kHz); c – obtained with proposed algorithm using 4 filters (ΔB=75 kHz))**

TABLE2. **The main parameters of the reconstructed phase velocity dispersion curves of the A_0 mode obtained in experimental investigation**

Filter bandwidth ΔB, kHz	Number of filters K	Central frequency, kHz		Frequency range, kHz	Band width, kHz	Band width, %
		1th filter	*Kth* filter			
25	10	20	200	25-200	175	88
50	5	30	180	30-160	130	65
75	4	35	185	50-150	100	50

So, it can be seen from the graphs Fig. 7 and data in Table 2 that using proposed hybrid technique the phase velocity dispersion curve is reconstructed in frequency ranges of different sizes and coverage from 50 to 88 % of the original signal bandwidth. When using narrowest filter bandwidth of 25 kHz, the A_0 mode phase velocity dispersion curve is reconstructed in wider frequency range compared with other.

As presented in previous work [28] narrower filter bandwidth increase the sensitivity of the signal technique to the frequency components with small amplitudes. The frequency components having smaller amplitudes are distributed in the beginning and in the end of the frequency spectrum Fig. 6(b). Frequency components with higher amplitudes are filtered out when using narrow-band filter while frequency components having low amplitudes are exposed. Thus, the remaining frequency components with low amplitudes are extended, leading to the reconstructed phase velocity dispersion curve in a wide band-width. However, a larger amount of narrow-band filters are required to cover the entire spectrum of the signal to be analyzed, therefore the calculation time is prolonged. On the other hand, using the wide-band filters a small number of the filters is needed to cover the bandwidth of the signal but the phase velocity dispersion curve is reconstructed in a narrower frequency range. It means that the frequency

components having smaller amplitudes are missing and as well as a part of the information. Consequently, it is important to complete the calculations of the quantitative and quality characteristics of the proposed hybrid technique using filters of different bandwidths. These characteristics should show which narrow-band or wide-band filter bandwidth gives more reliable and accurate results and which filter bandwidth could be recommended to use in future applications.

III. EVALUATION OF THE METHOD ACCURACY

The presented method is a part of the whole measurement process, therefore during the assessment of its accuracy the key attention is focused on the complex estimation of measurement uncertainty. A variety of filter bandwidths (25 kHz, 50 kHz and 75 kHz) are selected and used for evaluation of the method characteristics. The steps of the procedure to evaluate the method metrological parameters are:

- Comparison of reference and calculated phase velocities of dispersion curves and evaluation of systematic errors.
- Identification of sources of the errors and data preparation for the calculation of standard uncertainty components.
- Calculation of a complete uncertainty budget or the combined uncertainty and the expanded uncertainty.

Every standard uncertainty is calculated as:

$$u_m(Y) \equiv |W_m| u(X_m), \tag{6}$$

where $W_m \equiv \partial f / \partial X_m$ is the absolute sensitivity coefficient (uncertainties budget table in Fig. 8, the fifth column), $u(X_m)$ is the standard uncertainty (uncertainties budget table in Fig. 8, the third column) that is obtained from repeated observations or is evaluated by scientific judgement based on information of possible variability of the measured value X_m (uncertainties budget table in Fig. 8, the second column) [40]. The combined standard uncertainty $u_c(c_{ph})$ (uncertainties budget table in Fig. 8, thelast value of the third column) calculation involves all standard uncertainty contributions $u(Y_m)$ (uncertainty budget table in Fig. 8, the sixth column). The GUM Workbench version 2.4.1.384 software is used for the combined uncertainty components processes and analyzes. The expanded uncertainty of each reconstructed frequency range has been calculated also using Monte Carlo simulation. Values of W_m *(*sensitivity coefficient*)*, X_m *(value)*, $u(X_m)$ (standard uncertainty), $u(Y_m)$ (uncertainty contribution), $u_c(c_{ph})$ (combined standard uncertainty) are given in uncertainty budget table of Fig. 8, in columns accordingly 5, 2, 3, 6, 3 (last value in the column).

The systematic error is assessed comparing the experimental measurements results with the theoretical dispersion curve calculated by the SAFE method. The mean values of the absolute error $\bar{\Delta}_{c_{ph}}$, the average standard deviation $\sigma_{\bar{\Delta}_{c_{ph}}}$ and the mean relative error $\bar{\delta}_{c_{ph}}$ are determined for each segment of the estimated phase velocity dispersion curve and separately for each used filter. The calculated results are listed in Table 3.

The mean value of the absolute error is calculated according:

$$\bar{\Delta}_{c_{ph}} = \frac{1}{M} \sum_{m=1}^{M} \left| c_{phm} - c_{ph}^{SAFE} \right|, \tag{7}$$

where M is the number of points in a segment of the reconstructed dispersion curve,m^{th} – the point of experimentally reconstructed dispersion curve, c_{phm} is the phase velocity of the experimentally reconstructed dispersion curve, c_{ph}^{SAFE} is the phase velocity calculated using the SAFE method at the same frequency values.

The average standard deviation is calculated according:

$$\sigma_{\bar{\Delta}_{c_{ph}}} = \sqrt{\frac{\sum_{m=1}^{M} \left(c_{phm} - c_{ph}^{SAFE} \right)^2}{M \cdot (M-1)}}. \tag{8}$$

The mean relative error is equal to:

$$\bar{\delta}_{c_{ph}} = 100\,\% \cdot \frac{1}{M} \sum_{m=1}^{M} \frac{\left| c_{phm} - c_{ph}^{SAFE} \right|}{c_{ph}^{SAFE}}. \tag{9}$$

TABLE3. The mean values of the absolute and relative errors and the average standard deviations of the dispersive curves for separate filter bandwidth

Velocity value for A_o mode, c_{ph}	Filter bandwidth, kHz	Number of filters	Mean absolute error $\bar{\Delta}_{c_{ph}}$, m/s	Average standard deviation $\sigma_{\bar{\Delta}_{c_{ph}}}$,m/s	Mean relative error (systematic) $\bar{\delta}_{c_{ph}}$, %
1152 m/s	25	10	20.5	4.8	1.8
	50	5	24.8	8.2	2.2
	75	4	28.3	10.4	2.5

The various factors such as: the measuring equipment, the object mechanical and geometrical parameters, the environment, the measurement technique and others influence each other the measurement results. The measurements were performed in a laboratory at a controlled environment temperature (20±2) ºC. Based on the prior work [37], where the contact measurement method at sufficiently short distance 500 mm is used and the temperature changes do not constitute more than 2% of the overall uncertainty. Therefore, this parameter may be neglected.

Research has allowed highlighting the following sources of the combined uncertainty: the reconstruction of phase velocities dispersion curves, uncorrected error for frequency range, the scanner step, material properties of the object and thickness of the test sample.

It is then important to evaluate accuracy of the proposed technique in the entire reconstructed phase velocity dispersion curve segment. Which means, the maximum deviation from the average error for one point across the frequency range is included in total uncertainty [37]? To show the limits of the actual variability of the obtained

This article has been accepted for publication in a future issue of this journal, but has not been fully edited. Content may change prior to final publication. Citation information: DOI 10.1109/ACCESS.2020.2974586, IEEE Access

results the difference between limit value of absolute error and mean absolute error are calculated:

$$\Delta_{c_{\mathrm{phmax}}} = \max\left(\Delta_{c_{\mathrm{ph}m}} - \bar{\Delta}_{c_{\mathrm{ph}}}\right). \quad (10)$$

Accordingly, the obtained results for the different filter bandwidths 25 kHz, 50 kHz and 75 kHz are equal to 32.5 m/s, 41.2 m/s and 7.7 m/s. Then the standard uncertainty can be calculated as follows (it is assumed a normal distribution):

$$u\left(\Delta_{c_{\mathrm{phmax}}}\right) = \frac{\Delta_{c_{\mathrm{phmax}}}}{3}. \quad (11)$$

The estimated standard uncertainties are 10.8 m/s, 13.7 m/s and 2.6 m/s respectively for the different filter bandwidths 25 kHz, 50 kHz and 75 kHz (values are given in Fig. 8, column 3 of uncertainty budget table). This component corresponds to the estimated fluctuations of the Lamb wave frequency *f*, which is directly affected by the characteristics of the receiver [37].

When using the same measuring instruments to realise the techniques (instruments for environmental control and ultrasound system "*Ultralab*"), the scanning step of the scanner, transducer and object characteristics influence the phase velocity measurement results [37], [38].

The difference between two neighbouring points at which signals are received is $l = 0.5$ mm. The distance was determined with the standard uncertainty of 0.006mm. The sensitivity coefficient $W_{\Delta l}$ is equal to $1/t$, where t is the rectangular single pulse duration 3.85 µs. The dimension $\partial f/\partial \Delta_l u(\Delta_l)$ has considered the uncertainty of scanner step which is a component of the total standard uncertainty.

The thickness of test sample is 4mm and its variation Δd is assumed to be equal to ±0.0001m. Based on this information, the absolute standard uncertainty can be calculated using rectangular distribution: $u(\Delta_d) = \pm\frac{\Delta_d}{\sqrt{3}}$ (Fig. 8, column 3 of the uncertainty budget table).

Changes of phase velocity depend on the change of elastic constants. There are six independent elastic constants for characterization of the materials and their values are presented in Table 1: Density, Young's modulus in longitudinal E_1 and transverse E_2 directions, Poisson's rations in longitudinal ν_{12} and transverse ν_{23} directions and shear modulus in both longitudinal and transverse directions G_{12}. Their standard uncertainties and sensitivity coefficients are calculated using the methodology described in the previous article [37] and presented in Fig. 8. Each elastic constant is changed 20% except the density, which is specified by the manufacturer. The phase velocity is not been influenced by the E_2, ν_{12}, ν_{23} changes. The Young's modulus E_1 changes are incited a maximum change of phase velocity Δc_{ph}=*30m/*s. The changes of the shear modulus G_{12} caused a maximum change of phase velocityΔc_{ph}=*83m/s.* A rectangular distribution is used for all calculations of standard uncertainties related to plate materials characteristics.

A complete uncertainty budget is determined for each filter. The results of the combined and expanded uncertainties calculations are presented in Fig. 8. The Δl_l, Δl_d, Δl_{cphmax}, $\Delta l_{E1}\Delta l_{G12}$ corrections, but not their uncertainties, are estimated to be zero. It is assumed that the accuracy of the phase velocity measurement will not be depreciated by the uncertainties of E_2, ν_{12}, ν_{23}, ρ.

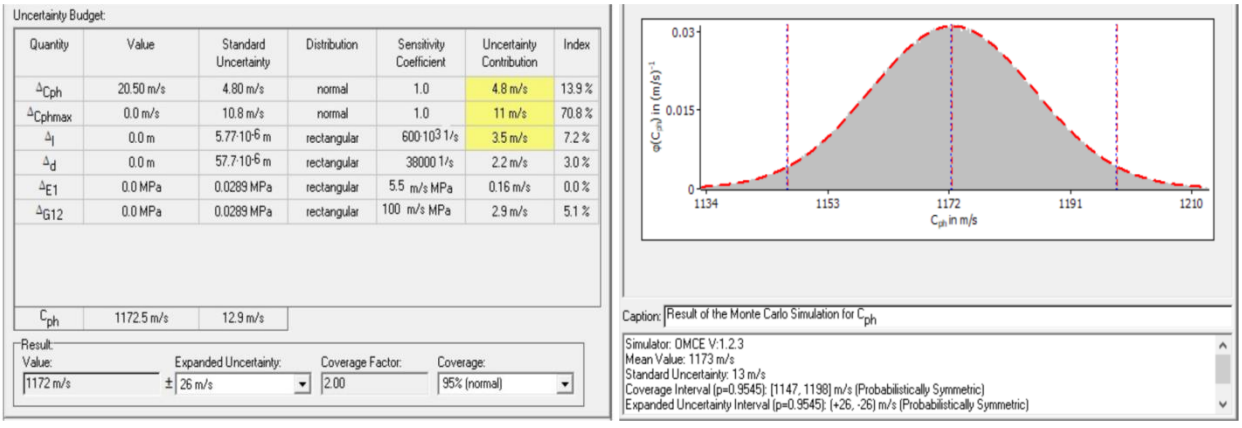

a

This article has been accepted for publication in a future issue of this journal, but has not been fully edited. Content may change prior to final publication. Citation information: DOI 10.1109/ACCESS.2020.2974586, IEEE Access

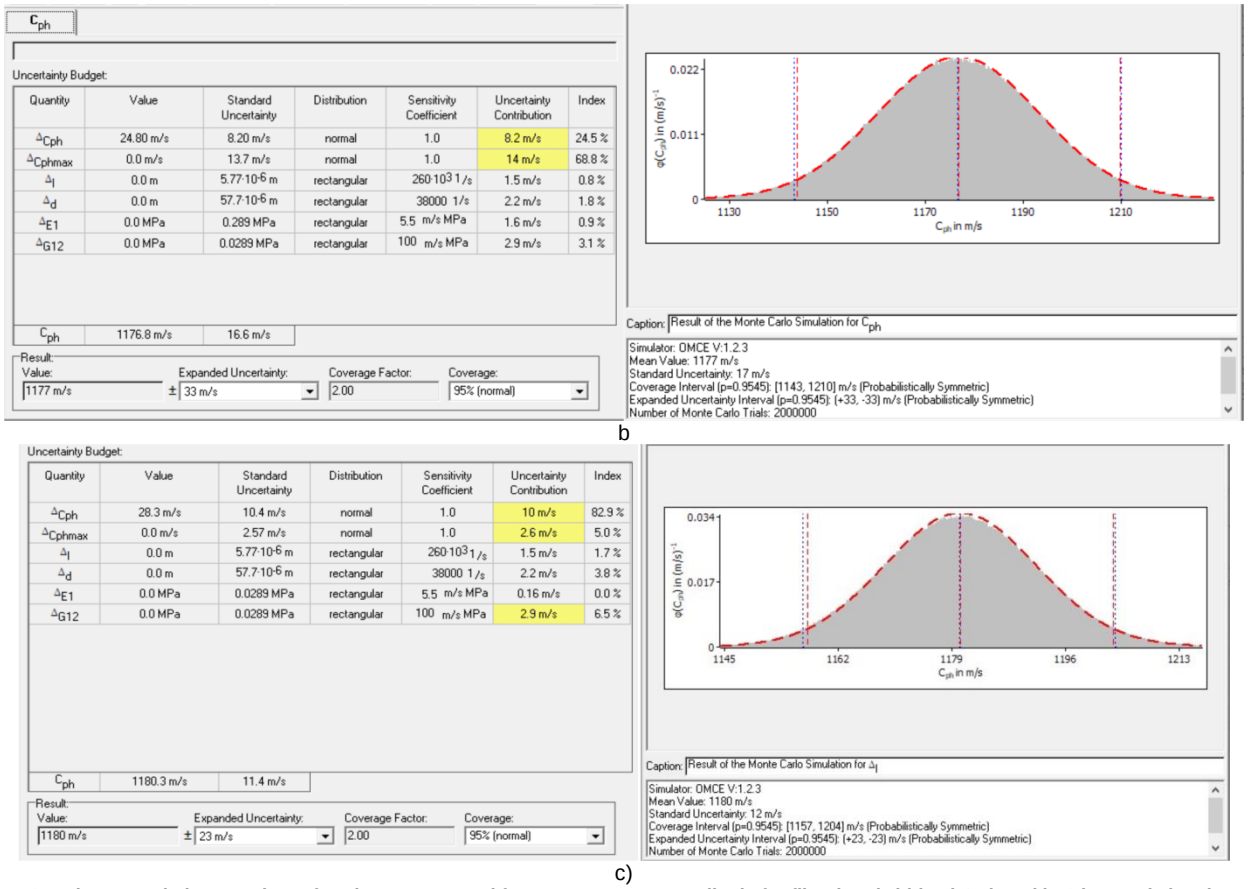

FIGURE 8. **The expanded uncertainty of each reconstructed frequency range accordingly for filter bandwidth: a) 25 kHz, b) 50 kHz and c) 75 kHz.**

The phase velocity measurement results are presented in Table 4. The expanded measurement uncertainty is calculated using the coverage factor p=2 for normal distribution and coverage probability P=0.95. When using narrower filter bandwidth 25 kHz, the reconstructed frequency range is wider (Table 2) and the typical error obtained is of 1.8% mean (Table 4). While using the wider filter bandwidth 75 kHz, the frequency range of the reconstructed dispersion curve is narrower (Table 2) and the typical error is larger and it of 2.5 % mean (Table 4).

TABLE4. **Calculated relative systematic errors and expanded uncertainties of the phase velocity for different filters.**

Filter bandwidth, kHz	Phase velocity c_{ph} for A_o mode, m/s	Mean relative error (systematic), %	Expanded relative uncertainty, %
25	1173	1.8	2.2
50	1177	2.2	2.8
75	1180	2.5	1.9

The results obtained with Monte Carlo simulation corresponds to the results calculated in the usual way. In all cases, there are positive systematic errors. Uncertainty analysis of these measurement results has shown that the main components of the combined standard uncertainty are the reconstruction of phase velocities dispersion curves and the uncorrected error for frequency range. The combined uncertainty of the phase velocity determination is also sensitive to the uncertainties of the scanner step and of the shear modulus which depends on the material properties of the object. The uncertainty of the shear modulus becomes significant when the uncertainty of the uncorrected error for frequency range decreases. The influence of the other uncertainty components to the measurement result will enhance accordingly.

The repeatability of the method or repeatability of the variation of the measured points of dispersion curves is a part of the combined standard uncertainty and is equal in the best case approximately to 14%. At the same time the reliability of the method in the whole segment of the phase velocity dispersion curve the maximum deviation from the average phase velocity error is included in the total standard uncertainty. The influence of uncertainties of the dispersion curve reconstruction and the uncorrected error for frequency range on the measurement result are evident and dominant. The two components represent 85% of the total uncertainty. The influence of other uncertainty components on the measurement result shall increase when these two uncertainties decrease. Ignoring these small components for uncertainty calculation can damage the quality of decision-making. It is important to take into account the changes in uncertainty, if the measuring equipment or object material is changed.

IV. CONCLUSIONS

The reliability characteristics of the proposed hybrid technique for the phase velocity estimation of Lamb wave A_0 mode were calculated and presented in this study. The experimental signals propagating in an anisotropic-non-homogeneous Glass Fibre Reinforced Plastic (GFRP) plate were used. To obtain the reliability characteristics of the method and to compare the obtained results, three different filter bandwidths 25 kHz, 50 kHz, 75 kHz were used in the investigation. Therefore, the obtained reconstructed dispersion curve segments have covered the different frequency range sizes with different mean systematic error. When using the narrower filter bandwidth 25 kHz, the phase velocity dispersion curve was reconstructed essentially in wider frequency range which covers 88%. In the meantime when using 75 kHz only 50% coverage of the whole incident signal frequency bandwidth was achieved. The evaluated characteristics have shown that the narrower filters bandwidth gives smaller measurement errors. Using 25 kHz filter bandwidth mean systematic error was equal to 1.8%, while in 75 kHz the error was 2.5%. The narrow-band filters provided more reliable and accurate results and also a reconstruction of dispersion curve segment in wider band. Therefore, it is recommended to use narrow-band filter for the Lamb waves A_0 mode phase velocity dispersion curve reconstruction.

REFERENCES

[1] L. Zeng, J. Lin, J. Bao, R. P. Joseph, and L. Huang, "Spatial resolution improvement for Lamb wave-based damage detection using frequency dependency compensation," J. Sound Vibr., vol. 394, pp. 130-145, 2017, https://doi.org/10.1016/j.jsv.2017.01.031.

[2] F. Gao, L. Zeng, J. Lin, and Y. Shao, "Damage assessment in composite laminates via broadband Lamb wave," Ultras., vol. 86, pp. 49-58, 2018, https://doi.org/10.1016/j.ultras.2018.01.005.

[3] N. Mori, S. Biwa, and T. Kusaka, "Damage localization method for plates based on the time reversal of the mode-converted Lamb waves," Ultras., vol. 91, pp. 19-29, 2019, https://doi.org/10.1016/j.ultras.2018.07.007.

[4] N. P. Yelve, M. Mitra, and P. M. Mujumdar, "Detection of delamination in composite laminates using Lamb wave based nonlinear method," Comp. Struct., vol. 159, pp. 257-266, 2017, https://doi.org/10.1016/j.compstruct.2016.09.073.

[5] L. Huang, L. Zeng, J. Lin, and Z. Luo, "An improved time reversal method for diagnostics of Liping composite plates using Lamb waves," Comp. Struct., vol. 190, pp. 10-19, 2018, https://doi.org/10.1016/j.compstruct.2018.01.096.

[6] Z. Tian, L. Yu, and C. Leckey, "Delamination detection and quantification on laminated composite structures with Lamb waves and wavenumber analysis," J. intell. mater. syst. struct., vol. 26, no. 13, pp. 1723–1738, 2015, https://doi.org/10.1177%2F1045389X14557506.

[7] K. A. Tiwari and R. Raisutis, "Identification and Characterization of Defects in Glass Fiber Reinforced Plastic by Refining the Guided Lamb Waves," Materials., vol. 11, no. 7, pp. 1-23, 2018, https://doi.org/10.3390/ma11071173.

[8] N. Toyama, J. Noda, and T. Okabe, "Quantitative damage detection in cross-ply laminates using Lamb wave method," Compos Sci. Technol., vol. 63, no. 10, pp. 1473-1479, 2003, https://doi.org/10.1016/S0266-3538(03)00163-5.

[9] K. Diamanti, C. Soutis, and J. M. Hodgkinson, "Lamb waves for the non-destructive inspection of monolithic and sandwich composite beams," Compos. Pt. A-Appl. Sci. Manuf., vol. 36, pp. 189-195, 2005, https://doi.org/10.1016/j.compositesa.2004.06.013.

[10] V. Giurgiutiu and M. F. Haider, "Propagating, Evanescent, and Complex Wavenumber Guided Waves in High-Performance Composites," Materials., vol. 12, no. 2, 269, pp. 1-31, 2019, https://doi.org/10.3390/ma12020269.

[11] R. Raisutis, R. J. Kazys, L. Mazeika, E. Zukauskas, V. Samaitis, L. Draudviliene, and A. Vladisauskas, "An adjustment-free NDT technique for defect detection in multilayered composite constructions using ultrasonic guided waves," Int J Struct Stab Dy., vol. 14, no. 8, pp. 1-15, 2014, https://doi.org/10.1142/S0219455414400252.

[12] Z. Su, L. Ye, and Y. Lu, "Guided Lamb waves for identification of damage in composite structures: a review," J. Sound. Vib., vol. 295, pp. 753–780, 2006, https://doi.org/10.1016/j.jsv.2006.01.020.

[13] C. Garnier, M. L. Pastor, F. Eyma, and B. Lorrain, "The detection of aeronautical defects in situ on composite structures using Non Destructive Testing," Compos. Struct., vol. 93, pp. 1328-1336, 2011, https://doi.org/10.1016/j.compstruct.2010.10.017.

[14] B. YangFu-Zhen, X. ChenShaoping, Z. Yang, and G. Xiao, "Damage localization and identification in WGF/epoxy composite laminates by using Lamb waves: Experiment and simulation," Compos. Struct., vol. 165, pp. 138-147, 2017, https://doi.org/10.1016/j.compstruct.2017.01.015

[15] S. Shoja, V. Berbyuk, and A.Bostrom, "Delamination detection in composite laminates using low frequency guided waves: Numerical simulations," Compos. Struct., vol. 203, pp. 826-834, 2018, https://doi.org/10.1016/j.compstruct.2018.07.025

[16] P. D. Wilcox, M. J. S. Lowe, and P. Cawley, "The effect of dispersion on long-range inspection using ultrasonic guided waves," NDT&E Int., vol. 34, no. 1, pp. 1–9, 2001, https://doi.org/10.1016/S0963-8695(00)00024-4.

[17] P. D. Wilcox, M. J. S. Lowe, and P. Cawley, "Mode and transducer selection for long range Lamb wave inspection," J. Int. Mater. Syst. Struct., vol. 12, pp. 553-565, 2001, https://doi.org/10.1177%2F10453890122145348.

[18] M. Voss, D. Ilseb, W. Hillgerb, T. Valléea, M. Eppmanna, J. de Witc and F. von Dungernc, "Numerical simulation of the propagation of Lamb waves and their interaction with defects in C-FRP laminates for non-destructive testing," Adv. Compos. Mater., pp. 1-19, 2019, http://dx.doi.org/10.1080/09243046.2019.1692273.

[19] F. Li, G. Meng, L. Ye, Y. Lu, and K. Kageyama, "Dispersion analysis of Lamb waves and damage detection for aluminum structures using ridge in the time-scale domain," Measure. Sci. Tech., vol. 20, pp. 1–10, 2009, http://dx.doi.org/10.1088/0957-0233/20/9/095704.

[20] B. Feng, A. L. Ribeiro, and H. G. Ramos, "Interaction of Lamb waves with the edges of a delamination in CFRP composites and a reference-free localization method for delamination," vol. 122, pp. 424-431, 2018, https://doi.org/10.1016/j.measurement.2017.10.016.

[21] J. L. Rose, "Back to Basics – Dispersion curves in guided wave testing," Mater. Eva., vol. 61, no. 1, pp. 20–22, 2003.

[22] J. Zou, J. Liu, and G. Tang, "Transverse spurious mode compensation for AlN Lamb wave resonators," IEEE Access., vol. 7, pp. 67059-67067, 2019, https://doi.org/10.1109/ACCESS.2019.2908340.

[23] A. Apostoloudia, E. Douka, L. J. Hadjileontiadis, I. T. Rekanos, and A. Trochidis, "Time-frequency analysis of transient dispersive waves: A comparative study," Appl. Acoust., vol. 68, pp. 296–309, 2007, https://doi.org/10.1016/j.apacoust.2006.02.002.

[24] P. D. Wilcox, "A rapid signal processing technique to remove the effect of dispersion from guided wave signals," IEEE Trans Ultrason Ferroelectr Freq Control, vol. 50, pp. 419-427, 2003, https://doi.org/10.1109/tuffc.2003.1197965.

[25] B. H. Crespo, C. R. P. Courtney, B. Engineer, "Calculation of Guided Wave Dispersion Characteristics Using a Three-Transducer Measurement System," Appl. Sci.-Basel., vol. 8, no. 8, pp. 1-15, 2018, https://doi.org/10.3390/app8081253.

[26] K. Thornicroft, C. Mares, and P. Mudge, "Time-frequency analysis of long range ultrasonic signals," J. Phys., Conf. Ser., vol. 382, pp. 1-6, 2012, https://doi.org/10.1088/1742-6596/382/1/012060.

[27] D. N. Alleyne and P. Cawley, "The interaction of Lamb waves with defects," IEEE Trans. Ultrason. Ferroelectr. Freq. Control., vol. 39, no. 3, pp 381–397, 1992, https://doi.org/10.1109/58.143172.

[28] L. Draudviliene, H. Ait Aider, O. Tumsys, and L. Mazeika, "The Lamb waves phase velocity dispersion evaluation using an hybrid

measurement technique," Comp. Struct., vol. 184, pp. 1156-1164, 2018, http://dx.doi.org/10.1016/j.compstruct.2017.10.060.

[29] J. Bai, Advanced Fibre-Reinforced Polymer (FRP) Composites for Structural Applications: 1. Introduction, Woodhead Publishing, Cambridge, UK, 2013. http://dx.doi.org/10.1533/9780857098641.1.

[30] J. M. Stickel and N. Mala, "Glass Fiber-Reinforced Composites: From Formulation to Application," Int. J. Appl. Glass Sci., vol. 3, pp. 122–136, 2012, https://doi.org/10.1111/j.2041-1294.2012.00090.x.

[31] M. Mrazova, "Advanced composite materials of the future in aerospace industry," INCAS Bull., vol. 5, pp. 139–150, 2013, http://dx.doi.org/10.13111/2066-8201.2013.5.3.14.

[32] T. Hayashi, S. Won–Joon, and J. L. Rose, "Guided wave dispersion curves for a bar with an arbitrary cross-section, a rod and rail example," Ultras., vol. 41, no. 3, pp. 175–183, 2003, https://doi.org/10.1016/S0041-624X(03)00097-0.

[33] P. Pollack, L. Yu, M. A. Sutton, S. Guo, P. Majumdar, M. Gresil, "Full-field measurements for determining orthotropic elaestic parameters of woven glass-epoxy composite using off-axis tensile specimens," Exp. Tech., vol. 38, no. 4, pp. 61-71, 2014, https://doi.org/10.1111/j.1747-1567.2012.00824.x.

[34] S. Ryan, M. Wicklein, A. Mouritz, W. Riedel, F. Schafer, and K. Thoma, "Theoretical prediction of dynamic composite material properties for hypervelocity impact simulations," Int. J. Impact Eng., vol. 36, pp. 899–912, 2009, https://doi.org/10.1016/j.ijimpeng.2008.12.012.

[35] L. Draudviliene, R. Raisutis, E. Zukauskas, and A. Jankauskas, "Validation of Dispersion Curve Reconstruction Techniques for the A0 and S0 Modes of Lamb Waves," Int. J. Str. Stab. Dyn., vol. 14, no 07, pp. 1-11, 2014, https://doi.org/10.1142/S0219455414500242.

[36] L. Draudviliene and L. Mazeika, "Investigation of the spectrum decomposition technique for group velocity measurement of Lamb waves propagating in CFRP composite plate," Electr. Electric. Engin., vol. 19, no. 2, pp. 57–60, 2013, https://doi.org/10.5755/j01.eee.19.2.3470.

[37] L. Draudviliene, A. Meskuotiene, L. Mazeika, and R. Raišutis, "Assessment of quantitative and qualitative characteristics of ultrasonic guided wave phase velocity measurement technique," J. Nondestruc. Eval., vol. 36, no. 2, pp. 1-13, 2017, https://doi.org/10.1007/s10921-017-0404-x.

[38] L. Draudviliene, A. Meskuotiene, R. Raišutis, and H. Ait Aider, "The Capability Assessment of the Spectrum Decomposition Technique for measurements of the Group Velocity of Lamb Waves," J. Nondestruc. Eval., vol. 37, no 2, pp. 1-13, 2018, https://doi.org/10.1007/s10921-018-0484-2.

[39] P. He, "Simulation of ultrasound pulse propagation in lossy media obeying a frequency power law," IEEE Trans. Ultrason. Ferroelectr. Freq. Control., vol. 45, pp. 114–125, 1998, https://doi.org/10.1109/58.646916.

[40] "Evaluation of measurement data" in *Guide to the expression of uncertainty in measurement*, BIPM, JCGM, pp. 1-134, 2008.

Lina Draudviliene received M.Eng. Degree in telecommunication engineering and a Ph.D. degree in measurements engineering from Kaunas University of Technology, Lithuania, in 2008 and 2012 respectively. From 2008 she worked as an engineer at Ultrasound Research Institute of Kaunas University of Technology then as a junior researcher. Since 2014 she is a researcher at Ultrasound Research Institute. Her research interests include ultrasonic guided waves measurements, non-destructive testing, structural health monitoring, material characterization and signal processing. She is the co-author over 20 scientific papers.

Asta Meskuotiene received M.Eng. Degree in mechanic engineering and a Ph.D. degree in measurements engineering from Kaunas University of Technology, Lithuania, in 1995 and 2002 respectively. From 2002 she worked as an engineer at Institute of Metrology of Kaunas University of Technology then as a researcher. Since 2008 she is a senior researcher at Institute of Metrology. She is technical expert of the National Accreditation Bureau, member of technical committee No. 34 "Metrology" of the Lithuanian Standards Board, member of the Metrology Expert Council of the National Metrology Institute. Her research interests include mass, pressure, density, length, volume measurements and signal processing, development of the traceability system of above mentioned measurement quantities, development of verification and calibration methods and expertise, Quality infrastructure system.

Olgirdas Tumšysreceived the Ing. Degree in electronics in 1986from the Kaunas Polytechnic Instituteand gained a Ph.D. degree in metrology and measurements from Kaunas University of Technology in 1995. Since year 1986 he has been employed as a research scientist at the Ultrasound Institute. His research interests include ultrasonic measurements, non-destructive testing and signal processing. He is author or co-author over50 scientific papers.

Liudas Mazeika received the degree of engineer–mathematic in 1986 from the Kaunas Polytechnic Institute, Lithuania. From 1980 started to work in the Ultrasound Laboratory of Kaunas University of Technology and in 1986 gained Ph.D degree in the field of measurement of mechanical quantities. From 2009 is the professor in the department of telecommunications. Currently is the principal researcher and director of Ultrasound Research Institute in Kaunas University of Technology. The fields of an interest include ultrasonic measurements, non-destructive testing, modelling and signal processing. He is the author or co-author over 100 scientific papers.

Vykintas Samaitis received M.Eng. Degree in measurements engineering and a Ph.D. degree from Kaunas University of Technology, Lithuania, in 2012 and 2016 respectively. From 2010 he worked as an engineer at Ultrasound Research Institute of Kaunas University of Technology initially and then successfully as a junior researcher. He has hands-on experience on a wide variety of projects including but not limited to ultrasonic inspection of adhesive joints, sprinkler pipes and composites. Since 2016 he is a researcher at non-destructive testing research group at Ultrasound Research Institute. His current interests include long-range guided wave inspection, structural health monitoring, material characterization, numerical modelling and signal processing.